Ca^{2+} channels at the plasma membrane of stomatal guard cells are activated by hyperpolarization and abscisic acid

David W. A. Hamilton, Adrian Hills, Barbara Köhler, and Michael R. Blatt*

Laboratory of Plant Physiology and Biophysics, Imperial College of Science, Technology, and Medicine, Wye, Kent TN25 5AH, England

Communicated by Enid MacRobbie, University of Cambridge, Cambridge, United Kingdom, February 16, 2000 (received for review August 25, 1999)

In stomatal guard cells of higher-plant leaves, abscisic acid (ABA) evokes increases in cytosolic free Ca^{2+} concentration ($[Ca^{2+}]_i$) by means of Ca^{2+} entry from outside and release from intracellular stores. The mechanism(s) for Ca^{2+} flux across the plasma membrane is poorly understood. Because $[Ca^{2+}]_i$ increases are voltage-sensitive, we suspected a Ca^{2+} channel at the guard cell plasma membrane that activates on hyperpolarization and is regulated by ABA. We recorded single-channel currents across the *Vicia* guard cell plasma membrane using Ba^{2+} as a charge-carrying ion. Both cell-attached and excised-patch measurements uncovered single-channel events with a maximum conductance of 12.8 ± 0.4 pS and a high selectivity for Ba^{2+} (and Ca^{2+}) over K^+ and Cl^-. Unlike other Ca^{2+} channels characterized to date, these channels rectified strongly toward negative voltages with an open probability (P_o) that increased with $[Ba^{2+}]$ outside and decreased roughly 10-fold when $[Ca^{2+}]_i$ was raised from 200 nM to 2 μM. Adding 20 μM ABA increased P_o, initially by 63- to 260-fold; in both cell-attached and excised patches, it shifted the voltage sensitivity for channel activation, and evoked damped oscillations in P_o with periods near 50 s. A similar, but delayed response was observed in 0.1 μM ABA. These results identify a Ca^{2+}-selective channel that can account for Ca^{2+} influx and increases in $[Ca^{2+}]_i$ triggered by voltage and ABA, and they imply a close physical coupling at the plasma membrane between ABA perception and Ca^{2+} channel control.

plasma membrane Ca^{2+} flux | cytosolic free Ca^{2+} oscillations | K^+ channel | inward rectifier | voltage clamp

Calcium ions are ubiquitous second messengers in living cells and contribute to physiological and developmental events in plants and animals (1–3). In plants, changes in cytosolic free Ca^{2+} concentration ($[Ca^{2+}]_i$) are associated with mechanical and thermal disturbances (3, 4), pathogen attack (5), and nodulation (6) and are central to hormonal physiology (7–9). Changes in $[Ca^{2+}]_i$ influence ion channel gating (1, 9, 10), light-mediated gene expression (11), cell differentiation, elongation, and tip growth (3).

In stomatal guard cells, one of the best-characterized plant cell models, increasing $[Ca^{2+}]_i$ is known to inactivate inward-rectifying K^+ channels and to activate Cl^- channels, biasing the plasma membrane for solute efflux, which drives stomatal closure (9). Changes in $[Ca^{2+}]_i$ have been associated with stimuli that lead to stomatal closure, notably abscisic acid (ABA) and CO_2 (9, 12). These changes in $[Ca^{2+}]_i$ depend on Ca^{2+} release from intracellular stores (13–16) and on Ca^{2+} entry across the plasma membrane (17, 18). Nonetheless, direct evidence for channels that could mediate Ca^{2+} influx has been lacking. Indeed, little evidence has come forth for Ca^{2+} channels at the plasma membrane of higher-plant cells until recently (19–23).

One clue to a major pathway for Ca^{2+} entry into guard cells has come from measurements of $[Ca^{2+}]_i$ and its elevation by ABA under voltage clamp (17). These studies indicated a voltage dependence to the $[Ca^{2+}]_i$ rise, suggesting that ABA stimulated a Ca^{2+} channel, but that its activity also required membrane hyperpolarization. We have recorded single-channel currents from *Vicia* guard cell protoplasts under conditions that eliminate the background of current through K^+ and Cl^- channels. The results reported here demonstrate the presence of Ca^{2+} channels at the plasma membrane that open on membrane hyperpolarization and are activated by ABA.

Materials and Methods

Plant Material. Epidermal strips of *Vicia faba* L., cv. Bunyard Exhibition, were obtained and protoplasts were prepared as described (24, 25). All operations were carried out on a Zeiss Axiovert microscope with 40× LWD Nomarski DIC optics at 20–22°C. Solution was added (≃20 chamber vol/min) by gravity feed and removed by aspiration.

Electrophysiology. Pipettes were pulled with a Narishige (Tokyo) PP-81 puller modified for three-stage pulls (input resistances, 30–50 MΩ) to reduce the number of channels under a patch. Pipettes were coated with Sigmacote (Sigma) to reduce capacitance. Connections to amplifier and bath were by a 0.1 M KCl/Ag–AgCl liquid junctions, and junction potentials were taken into account (26). Single-channel currents were recorded with an Axopatch 200B patch amplifier (Axon Instruments, Foster City, CA) after filtering at 5 kHz and sampled at 44 kHz for analysis. Data were filtered at 1 kHz (Kemo, Beckenham, U.K.) offline and analyzed with N-PRO (Wye Science, Wye, Kent, U.K.), P/V CLAMP V. 6 (CED, Cambridge, U.K.) software. Channel amplitudes were calculated from point-amplitude histograms estimated from open events ≥5-ms duration (Fig. 1) beyond closed levels determined from periods of no channel activity (27). Channel numbers were estimated from the maximum number of concurrent openings and from binomial distributions of open events (28). Channel openings were taken as transitions above thresholds of 60% of the single-channel amplitudes and open probability, P_o, was estimated from the open-time fraction corrected for the number of channels. Voltages quoted are referenced to the physiological orientation of the membrane, the voltage on the cytosolic side relative to the extracellular side.

Chemicals and Solutions. We use the terms "inside" and "outside" with reference to the physiological sidedness of the membrane. Protoplasts were normally bathed in 2, 10, and 30 mM Ba^{2+}-Hepes or Ca^{2+}-Hepes (pH 7.5) [Hepes buffer titrated to its pK_a with $Ba(OH)_2$ or $Ca(OH)_2$] adjusted to 200 mOsM with sorbitol, and pipettes were filled with similar solutions adjusted to 240 mOsM with sorbitol. Mg_2ATP at 1 mM was included in solutions

Abbreviations: $[Ca^{2+}]_i$, cytosolic free Ca^{2+} concentration; ABA, abscisic acid.

*To whom reprint requests should be addressed. E-mail: mblatt@wye.ac.uk.

The publication costs of this article were defrayed in part by page charge payment. This article must therefore be hereby marked "*advertisement*" in accordance with 18 U.S.C. §1734 solely to indicate this fact.

Article published online before print: *Proc. Natl. Acad. Sci. USA*, 10.1073/pnas.080068897. Article and publication date are at www.pnas.org/cgi/doi/10.1073/pnas.080068897

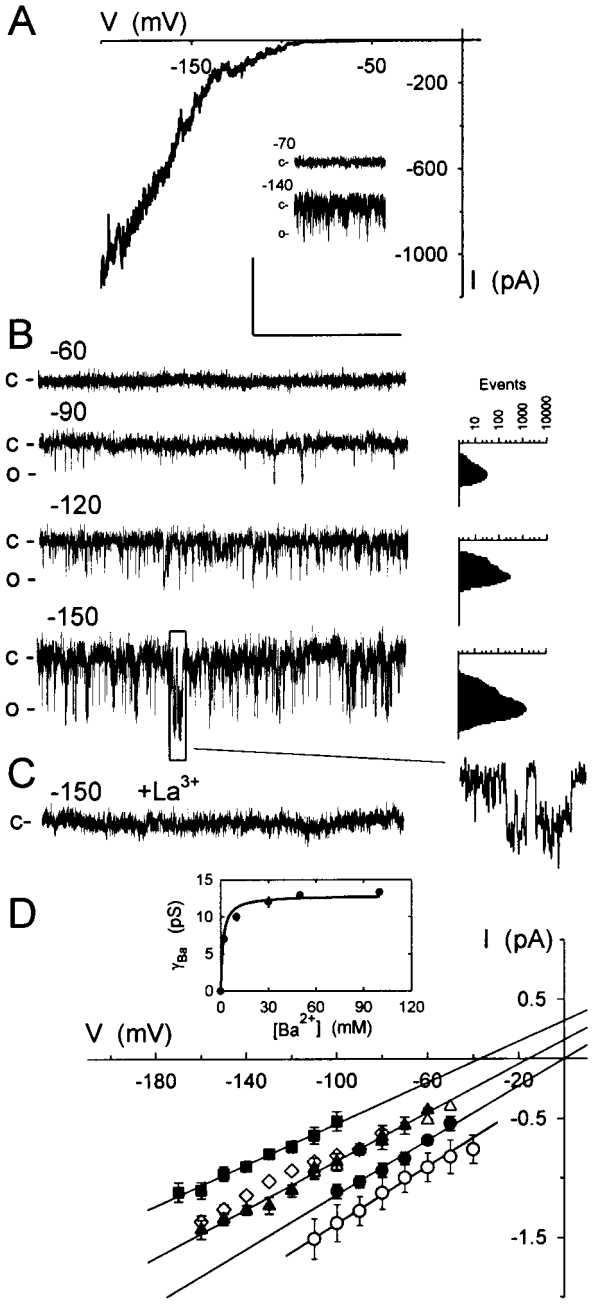

Fig. 1. Ca^{2+} channels at the plasma membrane of *Vicia* guard cells uncovered at negative voltages. (*A*) Representative whole-cell record with voltage clamped to a 30-s ramp from +50 to −200 mV with 30 mM Ba^{2+} in bath and 30 mM Ba^{2+} in the pipette. (*Inset*) Cell-attached records with voltages (in mV) calculated assuming that a protoplast voltage of −50 mV, close to the voltage obtained in whole-cell recordings with the current clamped to zero. (*B*) Current from one outside-out patch with 30 mM Ba^{2+} in the pipette (inside) and 10 mM Ba^{2+} in the bath. Voltages (*Left*) in mV. (*Insets*, *Right*) Point-amplitude histograms (27) used to estimate open-channel amplitudes (see *Methods*; note the log scale) and single-channel events at −150 mV shown on an expanded time scale. (*C*) Current from the same patch as in *B* after adding 100 μM $LaCl_3$ to the bath. Scale (*A–C*): vertical, 2 pA (*A*, *Inset*: 4 pA); horizontal, 1 s (*A*, *Inset*: 2 s; *B*, *Inset*: 150 ms). (*D*) Means ± SEM of open-channel currents from outside-out patches (n = 9) with 30 mM Ba^{2+} inside and 2 (■), 10 (▲), and 30 mM Ba^{2+} (●) outside. Currents from cell-attached patches (○, n = 8) as in *A* but with voltage uncorrected for comparison of γ_{Ba}. Regression analyses (lines) of these data extrapolated to the voltage axis to determine E_{rev}. Means ± SEM of currents from separate measurements with addition of 20 mM Cl^- as $BaCl_2$ (△, n = 5) and with 10 mM Ca^{2+} (◇, n = 4) in place of Ba^{2+} outside included for comparison. (*Inset*) γ_{Ba} plotted against $[Ba^{2+}]$ and fitted to a simple hyperbolic function.

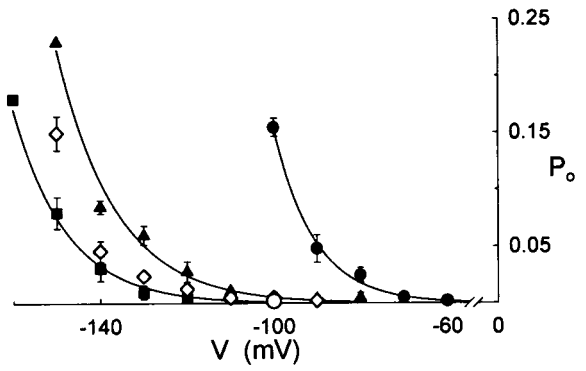

Fig. 2. Ca^{2+} channel open probability (P_o) is elevated by membrane hyperpolarization and $[Ba^{2+}]$ outside. Means ± SE of P_o from mean open times of 100-s recordings including data of Fig. 1 with 2 (■), 10 (▲), and 30 mM Ba^{2+} (●) outside, and with 10 mM Ca^{2+} (◇) in place of Ba^{2+} outside. Mean ± SE of measurements at −100 mV (n = 3) with 10 mM Ba^{2+} inside and 30 mM Ba^{2+} outside (○, compare ●) show the effect of changing $[Ba^{2+}]$ inside. Curves are empirical fittings to a common exponential function.

on the inside of the membrane. K^+ was added as K^+-Hepes (pH 7.5) [Hepes buffer adjusted to its pK_a with KOH] and Cl^- was added as $BaCl_2$. Ca^{2+} on the inside of the membrane was buffered with EGTA, and the final concentration was calculated according to Foehr *et al.* (29). ABA was prepared as a stock in ethanol and diluted ≥1,000-fold for use. Ethanol alone (0.1%) had no effect on the channels. Buffers, salts, and ABA were from Sigma.

Results

Guard Cells Harbor a Low-Conductance Channel Selective for Ca^{2+} and Permeable to Ba^{2+}. The activity of guard cell Cl^- channels is suppressed when the external anion concentration is reduced (30, 31). Guard cell K^+ channels are blocked by millimolar Ba^{2+}, and extracellular K^+ is required for channel activity of inward-rectifying K^+ channels and as a substrate (32). Because Ba^{2+} also permeates many Ca^{2+} channels (19, 33, 34), we reasoned that Ca^{2+} channels might be identified if initially Ba^{2+} was the only charge-carrying ion. Fig. 1 shows measurements obtained from guard cell protoplasts at different stages of patch excision. Driving the membrane to inside negative voltages uncovered channel events of low amplitude and flickering characteristic in cell-attached measurements and excised patches, and a strongly inward-rectifying current in whole-cell recordings (Fig. 1*A*). No channel openings or whole-cell currents were observed when the membrane was held near 0 mV or at voltages to +100 mV (not shown). Similar results were obtained in excised patches with voltage under direct experimental control, and on replacing Ba^{2+} with Ca^{2+} in the bath (Fig. 1 *B* and *D*). No evidence of rundown was observed in these experiments and during recordings of up to 82 min. Channel activity (and whole-cell current, not shown) was blocked by 100 μM Gd^{3+} or La^{3+} (Fig. 1*C*), regardless of whether Ba^{2+} or Ca^{2+} was present as the charge-carrying ion.

Open-channel current–voltage curves indicated that the divalent cations were the principal charge-carrying species passing through the channels (Fig. 1*D*). Because the channels opened only at negative voltages, the current reversal (equilibrium) voltage, E_{rev}, was obtained by extrapolation. These estimates were nonetheless in good agreement with the predicted equilibria and showed the expected positive-going shift in voltage with increasing Ba^{2+} in the bath. With 30 mM Ba^{2+} inside and 2, 10, and 30 mM Ba^{2+} outside, E_{rev} was −34 ± 2, −12 ± 3, and −1 ± 3 mV, respectively. Increasing $[Ba^{2+}]$ outside also increased the single-channel conductance for Ba^{2+} (γ_{Ba}), for a

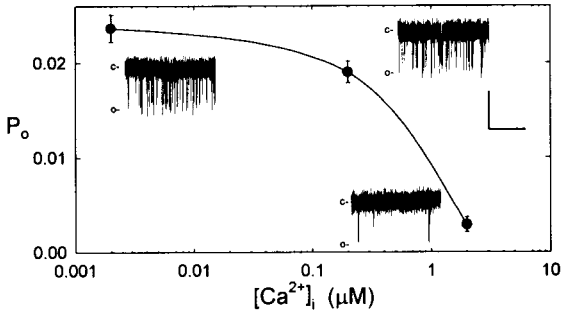

Fig. 3. P_o is suppressed by micromolar $[Ca^{2+}]_i$. Means ± SE of P_o from mean open times of 100-s recordings at −120 mV ($n = 3$). Ca^{2+} added on the cytosolic side (inside) during inside-out recordings against a background of 30 mM Ba^{2+} and with 10 mM Ba^{2+} outside. (*Insets*) Segments of traces at each $[Ca^{2+}]_i$. Data from one patch. Scale: vertical, 1 pA; horizontal, 1 s.

maximum γ_{Ba} of 12.8 ± 0.4 pS and a $K_{1/2}$ for γ_{Ba} of 1.6 ± 0.2 mM Ba^{2+} (Fig. 1*D*, *Inset*), and a similar conductance was obtained in cell-attached recordings (Fig. 1*D*). Replacing Ba^{2+} with Ca^{2+} gave virtually identical results (Fig. 1*D*, ◇), and replacing Ba^{2+}-Hepes with $BaCl_2$ (Fig. 1*D*, △) or including 5 mM K^+ as K^+-Hepes in the bath and pipette (not shown) had no measurable effect on the single-channel conductance or the current reversal voltage. With 10 mM Ca^{2+} outside, E_{rev} was −10 ± 4 mV, and including 20 mM Cl^- against a background of 10 mM Ba^{2+} gave E_{rev} of −9 ± 4 mV. With 5 mM K^+ and 2 mM Ba^{2+} outside, E_{rev} was −36 ± 5 mV, respectively. These results indicate roughly equal permeabilities to Ca^{2+} and Ba^{2+}, and a high selectivity (>10:1) for these ions over K^+ and Cl^-.

Ca^{2+} Channels Are Activated by Membrane Hyperpolarization and Extracellular Divalent Cations. Previous measurements of $[Ca^{2+}]_i$ (17) led us to suspect a steep dependence of channel opening on membrane voltage beyond about −100 mV. Calculated in consecutive 0.2- to 5-s segments showed P_o rose immediately ($\tau \leq$ 100 ms) on negative voltage steps (see Fig. 5, trace f). Therefore, to assess channel open probabilities (P_o), single channel events were recorded from excised, outside-out patches after stepping the membrane to selected voltages for periods of 100 s.† Fig. 2 summarizes results from experiments, including data from Fig. 1*B* and measurements with patches transferred between 2, 10, and 30 mM Ba^{2+} outside ($n = 6$). In 2 mM Ba^{2+} outside, P_o rose from values near 0.002 at −100 mV to 0.18 at −160 mV. P_o also rose with $[Ba^{2+}]$ outside at any one voltage with the effect that the voltage sensitivity for channel opening appeared displaced to the right along the voltage axis. The effect was most pronounced at $[Ba^{2+}]$ outside above 10 mM. A similar voltage dependence was observed with Ca^{2+} substituting for Ba^{2+} outside, although P_o was reduced in Ca^{2+} (Fig. 2), compared with the same concentration of Ba^{2+}.

Changing $[Ba^{2+}]$ on the inside of the membrane had a similar effect on P_o (see Fig. 2, ○). However, increasing $[Ca^{2+}]_i$ affected P_o conversely. Fig. 3 shows the results of measurements at −120 mV from inside-out patches with 10 mM Ba^{2+} outside and Ca^{2+} added against a background of 30 mM Ba^{2+} inside. Raising

†The true number of channels per cell is difficult to estimate, but is almost certainly greater than this value. Most patches showed one to three channel levels (<4% in total showed no Ca^{2+} channels), and as many levels again were uncovered in ABA. For this same reason, values given for P_o are probably overestimated in proportion. An underestimate of 2-fold in the channel number N introduces an error of 50% in the estimate for P_o (28). We have assumed an average of five channels (the mean in ABA), a patch area of 1 μm^2, a cell surface area of 1,000 μm^2 (17, 37), and values for P_o of 0.001 before and 0.1 after adding ABA. Total membrane current $I = \gamma_{Ca}(V - E_{Ca})NP_o$, where V is the membrane voltage and E_{Ca} is the Ca^{2+} equilibrium voltage.

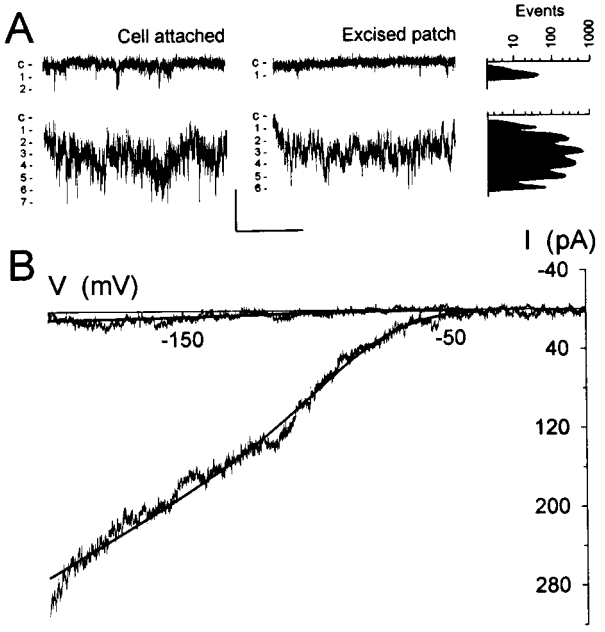

Fig. 4. ABA activates Ca^{2+} channels. (*A*) Records from two patches, cell-attached (*Left*) and excised inside-out (*Right*) before (*Top*) and after (*Bottom*) adding 20 μM ABA to the bath. Traces in ABA at 55 s (cell-attached) and 20 s (excised patch) after additions. Membrane voltage clamped to −100 mV and with 30 mM Ba^{2+} in bath and pipette (cell-attached) or with 30 mM Ba^{2+} inside and 10 mM Ba^{2+} outside (excised patch). Scale: vertical, 2 pA; horizontal, 1 s. Point-amplitude histograms of channel openings for excised patch data plotted on a log scale (*far right*): events −ABA taken over 100 s; events +ABA taken over 5 s and scaled by a factor of 20 for comparison. (*B*) Current–voltage curves obtained by summing currents recorded from one excised, inside-out patch during 10-s voltage ramps between 0 and −200 mV. Baseline (leakage) current corrected by subtracting corresponding data (−ABA) with no opening events. Data are the sum of 40 ramps (−ABA) and 10 ramps (+ABA) taken immediately before and after adding ABA. Sum before ABA addition scaled by 0.25 for comparison, and both current-voltage curves fitted to a Boltzmann function of the form

$$I = \frac{g_{max}\,(V - E_{Ba})}{1 + e^{\delta\, zF\,(V - V_{1/2})/RT}}, \qquad [1]$$

where g_{max} is the relative conductance maximum, V the clamp voltage, E_{Ba} the Ba^{2+} equilibrium voltage (= −14 mV), δ the voltage sensitivity factor, $V_{1/2}$ the voltage giving half-maximal current activation, and z, F, R, and T have their usual meanings. Fitted parameters (+ABA): δ, 0.93 ± 0.05; $V_{1/2}$, −83 ± 2 mV. Fittings of currents summed before adding ABA gave $V_{1/2}$, −142 ± 48 mV if δ was constrained to a value of unity. Variation in P_o (see Fig. 5) accounts for the lower activation by ABA when summed over 50 s.

$[Ca^{2+}]_i$ from 200 nM to 2 μM reduced P_o roughly 10-fold. Ba^{2+} often is a poor substitute for Ca^{2+} in binding/regulatory functions (33, 35, 36), and these results suggest that channel opening is subject to control by $[Ca^{2+}]_i$.

ABA Potentiates Ca^{2+} Channel Activity. ABA alters the voltage sensitivity of evoked increases in $[Ca^{2+}]_i$ (17), an observation that could be explained if the hormone affected the P_o of Ca^{2+} channels mediating Ca^{2+} influx across the plasma membrane. To test this idea, we replaced the standard bathing medium with medium containing ABA during recordings. Fig. 4*A* (*Left*) shows sections of a continuous recording from one cell-attached patch clamped near −100 mV. Before ABA exposure, the current trace was punctuated by occasional channel openings (upper trace). P_o calculated from the 100-s period immediately before adding ABA gave a value of 0.002. Within 60 s of adding 20 μM

ABA, the channel activity increased dramatically, consistent with at least seven channels in the patch (lower trace). P_o calculated from a 5-s period 60 s after ABA addition was 0.19, equivalent to a 93-fold rise over the value before ABA exposure. Similar results were obtained in six other independent experiments, giving a mean rise in P_o of 125-fold from 0.002 ± 0.0005 before to 0.25 ± 0.08 after adding ABA.

One difficulty with cell-attached measurements lies in the uncertainty about the membrane voltage (see Fig. 1, legend). In principle, the increase in P_o might have resulted either directly from an effect of ABA on Ca^{2+} channel gating or indirectly through a change in voltage. However, whereas Ca^{2+} channel opening is promoted by hyperpolarization (Fig. 2), the effect of ABA, if any, is to depolarize the membrane (32, 37). Hyperpolarizing the membrane would also be expected to increase open-channel current by virtue of the increase in electrical driving force. Yet, comparing open-channel currents before and after ABA treatments showed no significant difference in current amplitude or single-channel conductance, arguing for a direct effect of ABA on P_o rather than one mediated by a change in voltage.

To confirm this interpretation, we carried out recordings with excised, inside-out patches clamping the membrane to −100 mV. In each of four experiments, adding 20 μM ABA resulted in an immediate (<10-s lag time) increase in Ca^{2+} channel events (Fig. 4*A*, *Right*). Equivalent results were obtained in one recording from an outside-out patch, and in two inside-out patches with 0.1 μM ABA, with the difference that P_o rose first 110–205 s after adding ABA. In every case, the increase in P_o occurred without measurable change in γ_{Ba}. For the data shown, P_o calculated from the 100-s period immediately before adding ABA was 0.003. After 20 s in ABA, at least six channels could be identified in the patch (lower trace), and P_o calculated from a 5-s period was 0.55, equivalent to a 183-fold rise over the value before ABA exposure. For all seven experiments, the mean rise in P_o was 187-fold from 0.003 ± 0.0001 before to 0.56 ± 0.06 measured 30 s after adding ABA; γ_{Ba} and E_{rev}, respectively, were 9.8 ± 0.4 pS and 9 ± 3 mV before, and 9.3 ± 3 pS and 8 ± 2 mV after adding ABA.

We also clamped membrane patches driving the voltage in 5-s ramps between 0 and −200 mV, sufficiently long to ensure a P_o was at quasi-steady state throughout (see above and Fig. 5). Ramps yielding no channel activity were subtracted from these records to eliminate the baseline (leakage) current of the patch to examine the effect of ABA on the voltage sensitivity of channel activation. The resulting current-voltage curves were fitted to a Boltzmann function (Fig. 4) to estimate the voltage giving half-maximal activation, $V_{1/2}$. Fig. 4*B* shows results from one inside-out patch, 40 ramps sampled before and 10 ramps sampled immediately after adding 20 μM ABA. Before adding ABA, very little current was evident at voltages positive −120 mV, whereas in ABA an appreciable current was evident even at voltages near −50 mV. For the currents recorded in ABA, fitting gave a $V_{1/2}$ of −83 ± 2 mV. Best fittings for currents recorded before ABA addition gave a $V_{1/2}$ near −140 mV, but, because of the low signal level, this value should be seen as a rough estimate only. Comparable results were obtained in three other experiments. Thus, the analyses indicate a significant increase in current positive of −100 mV in the presence of ABA.

ABA Evokes Oscillations in Ca^{2+} Channel Open Probability. Both cell-attached and excised patch recordings showed that P_o rose transiently in ABA and that, even after washing 5–8 min without ABA, subsequent exposures failed to elicit a second rise in P_o. We also noted a delay in response to ABA in cell-attached recordings, whereas in inside-out patches the rise in P_o occurred roughly within the time required (≈5 s) for exchange of the bath solution. These observations suggested that elements necessary

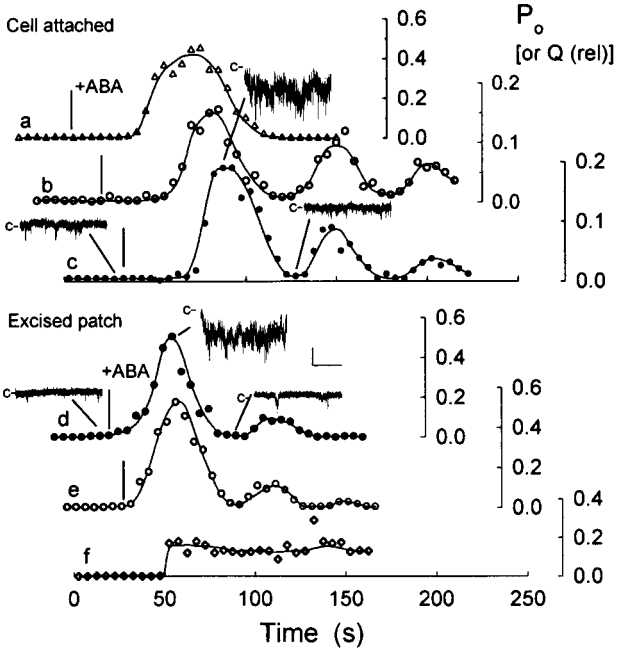

Fig. 5. ABA, but not voltage steps, evokes oscillations in Ca^{2+} channel activity. P_o (data points) and relative net charge, *Q* (solid lines), calculated at consecutive 5-s intervals in six independent experiments (a–f, three cell-attached, three excised, inside-out patches). Note the different P_o scales (*Right*) for each experiment. *Q* calculated by summing all points above the zero current level during each 5-s interval and scaled to P_o ranges. Segments of current traces c and d (including data from Fig. 4) with closed level (−c) as indicated. Scale: vertical, 2 pA; horizontal, 1 s. Times of ABA addition indicated (|, *Left*) in each experiment and aligned between c and e. Voltage stepped from −100 to −150 mV at 50 s in f.

for Ca^{2+} channel activation and its regulation by ABA were retained on the excised membrane, and raised a question about the temporal characteristics of response. To detail the time course of Ca^{2+} channel activation, we calculated P_o for consecutive 5-s segments of recordings before and during treatments with 20 μM ABA with the membrane clamped throughout at or near −100 mV. For comparison, similar calculations were carried out for voltage steps to −150 mV and using total charge, taken as the data-point amplitude sum above the closed-channel level. Fig. 5 shows measurements from six experiments (three cell-attached, three excised patches). In all but one case (Fig. 5, trace a), ABA exposures led to damped oscillations in P_o. Equivalent oscillations were seen in total charge (solid lines), so discounting possible errors in estimating P_o, channel number or γ_{Ba}. Both cell-attached and excised, inside-out recordings showed a similar period of oscillation near 50 s [means of (*n*) patches: cell-attached, 53 ± 6 s (5); inside-out, 55 ± 8 s (4)]. No oscillations were observed following voltage steps alone (Fig. 5, trace f). The initial rise of P_o in cell-attached measurements was delayed by 23–57 s (mean, 33 ± 4 s). For the inside-out patches, however, a significant increase in P_o was evident in every case during the first 5-s time segment after adding ABA.

Discussion

In guard cells, ABA evokes increases in $[Ca^{2+}]_i$ that depend in part on Ca^{2+} entry across the plasma membrane. Although a role for Ca^{2+} channels has been suggested (18, 38–40)—most recently based on the voltage sensitivity of evoked $[Ca^{2+}]_i$ increases (17)—direct evidence for such channels has been lacking. We now demonstrate that *Vicia* guard cells harbor a low-conductance Ca^{2+} channel at the plasma membrane that is

selective for Ca^{2+} (and Ba^{2+}) over K^+ and Cl^-, and is blocked by the Ca^{2+} channel antagonists Gd^{3+} and La^{3+} (Fig. 1). Channel open probability (P_o) was increased by membrane hyperpolarization, both in cell-attached and excised-patch recordings, and was favored by increasing divalent concentration outside (Fig. 2), whereas increasing $[Ca^{2+}]_i$ suppressed P_o (Fig. 3). Channel opening was strongly and transiently enhanced during exposures to ABA, leading to a significant current at voltages as positive as −50 mV (Fig. 4) and oscillations in P_o (Fig. 5). These results match the characteristics anticipated from measurements of $[Ca^{2+}]_i$ (17), and point to a close physical association between the Ca^{2+} channel and the site of perception for ABA.

A key feature of the Ca^{2+} channel is its activation by negative membrane voltage. Channel openings were extremely rare at voltages above −50 mV both in excised and, to a best estimate, in cell-attached patches. Channel openings were generally evident at voltages negative of −100 mV in 2 and 10 mM Ba^{2+} or Ca^{2+} outside, with P_o rising from values near 0.002 to 0.15–0.2 at −160 mV. The observations imply an appreciable Ca^{2+} influx only on membrane hyperpolarization and, thus, complement evidence of voltage-evoked changes in $[Ca^{2+}]_i$. Grabov and Blatt (17) reported increases in $[Ca^{2+}]_i$ that were triggered when the guard cell plasma membrane was hyperpolarized beyond a threshold near −120 mV. They showed that the rise in $[Ca^{2+}]_i$ depended on a voltage-triggered influx of Ca^{2+} and was sensitive to Gd^{3+}. Furthermore, they found that increasing $[Ca^{2+}]$ in the bath accelerated the rate of $[Ca^{2+}]_i$ rise during negative voltage steps, consistent with our present observation that P_o rose with $[Ba^{2+}]$ outside (Fig. 2). Thus, the characteristics of the Ca^{2+} channel match closely the properties anticipated from these earlier measurements of voltage-evoked $[Ca^{2+}]_i$ increases.

In fact, the sensitivity to negative voltages may be a common feature of plant plasma-membrane Ca^{2+} channels that effect $[Ca^{2+}]_i$ changes. Stoeckel and Takeda (41) reported an inactivation of K^+ channels in *Mimosa* that was relieved by Gd^{3+}, and proposed that Ca^{2+} channel activation at the plasma membrane triggered a rise in $[Ca^{2+}]_i$ to mediate this effect. Hyperpolarization-activated Ca^{2+}-permeable channels occur in tomato (19) and have been implicated in response to pathogen attack (20, 42). However, the acute voltage-sensitivity, high selectivity for Ca^{2+} over K^+ and Cl^-, and activation by ABA distinguish the present data from reports of a nonselective, Ca^{2+}-permeable channel (43) and of Ca^{2+} entry through K^+ channels (44). The guard cell Ca^{2+} channel also differs from depolarization-activated Ca^{2+} channels found in wheat roots (22) and carrot cell cultures (21).

A significant feature of the Ca^{2+} channel was its sensitivity to $[Ca^{2+}]_i$. Increasing $[Ca^{2+}]_i$ to 200 nM had little influence on P_o, but at 2 μM $[Ca^{2+}]_i$ reduced P_o by roughly 10-fold (Fig. 3). Because $[Ca^{2+}]_i$ normally lies near 200 nM *in vivo*, but on stimulation can rise to values above 1 μM (12, 15–17), this sensitivity of P_o implies a critical role of $[Ca^{2+}]_i$ in feedback regulation of the channel. Similar characteristics of $[Ca^{2+}]_i$ regulation are known for mammalian L-type Ca^{2+} channels and are associated with Ca^{2+} binding sites on the channel protein (45, 46).

Equally intriguing is the sensitivity of the Ca^{2+} channel gate to divalent cation concentration outside (Fig. 2), an effect that is distinct from any change in open-channel conductance. This action on P_o differs from that of $[Ca^{2+}]_i$, and suggests a unique divalent cation binding site outside that interacts with the channel gate with a $K_{1/2}$ above 10 mM. To our knowledge, these characteristics are without precedent among Ca^{2+} channels in plants and animals. For neuronal Ca^{2+} channels, limited increases in P_o have been reported with external $[Ca^{2+}]$, but are the effect of surface-charge masking and saturate below 2 mM $[Ca^{2+}]$ (36). The action of external Ca^{2+} and Ba^{2+} on the guard cell Ca^{2+} channel does show similarities to K^+ action on outward-rectifying K^+ channels in yeast (47) and many plant cells, including guard cells (32, 48). Whether the mechanism(s) of action are analogous remains to be determined.

Most remarkable was our finding of Ca^{2+} channel activation by ABA. Channel open probability increased in ABA by up to 210-fold in cell-attached recordings, by up to 260-fold in excised patches, paralleling total charge flux, Q (Figs. 4 and 5). This activation was transient and was accompanied by a profound increase in current at voltages positive of −100 mV. Again, these characteristics are anticipated from measurements of $[Ca^{2+}]_i$, which showed that ABA treatments displace the voltage threshold necessary to raise $[Ca^{2+}]_i$ (17). We noted also a significant delay before P_o rose when ABA was added to the bath in the cell-attached recordings. By contrast, P_o and Q rose without a measurable lag when ABA was added to the cytosolic side of the membrane in inside-out patches (Fig. 5). Little ABA in these measurements would have been present as the undissociated free acid ($pK_a = 4.7$) and, therefore, membrane permeable at pH 7.5. So, the observation is consistent with, although not proof of, ABA acting at a binding site on the inside of the membrane.

The predicted Ca^{2+} flux through the channel is plausibly sufficient to raise or trigger a rise in $[Ca^{2+}]_i$ in the presence of ABA. From the number of opening events evident in patches in the presence of ABA, we estimate that a *Vicia* guard cell harbors a minimum of 5,000 Ca^{2+} channels.† Given conditions of 1 mM Ca^{2+} outside, γ_{Ca} could be reduced to approximately 2 pS (Fig. 1, *Inset*), although with 1 μM $[Ca^{2+}]_i$ and a membrane voltage of −120 mV (17), the driving force for Ca^{2+} entry would be close to +220 mV. If we assume that P_o rises to 0.1 in ABA, then the total Ca^{2+} current calculated is 200 pA and the Ca^{2+} flux is 2 fmol·s^{-1}. For a guard cell with a cytosolic volume of 1 pl, this flux translates into a rate of rise in total cytosolic $[Ca^{2+}]$ close to 2 mM·s^{-1}. Even allowing for a static Ca^{2+} buffer content of 50 μM (49), this value is well in excess of what would be required to elevate $[Ca^{2+}]_i$. At the same time, the current would be masked by the background of K^+ and Cl^- currents in whole-cell measurements (37, 50) and, in the absence of ABA, the Ca^{2+} current (<2 pA) would not be resolved under these conditions.

Because the Ca^{2+} channels responded to ABA even in excised patches (Figs. 4 and 5), our data also point to a close physical association between site of ABA perception and the Ca^{2+} channel. One intriguing discovery was that P_o recovered to near-initial values through damped oscillations specific to the ABA stimulus (Fig. 5). ABA is known to evoke oscillations in $[Ca^{2+}]_i$ of guard cells (16), although these events may be coupled secondarily to oscillations in membrane voltage (17, 51). In fact, the oscillations in Ca^{2+}-channel P_o occurred with a period roughly an order of magnitude shorter than free-running oscillations in $[Ca^{2+}]_i$ reported in ABA and, therefore, alone cannot account for these phenomena. Nonetheless, the fact that the oscillations in P_o were observed in excised patches, and that subsequent exposures to ABA failed to evoke a response, points to a subtle mechanism that regulates the Ca^{2+} channel and indicates that this mechanism, and other elements of the ABA signal cascade, remain intact associated with the plasma membrane. We can rule out a direct role for $[Ca^{2+}]_i$ as a regulatory factor, because the oscillations were observed in excised patches and with Ba^{2+} (not Ca^{2+}) on both sides of the membrane. At present, the nature of these associations remains unknown, but are clearly of tremendous interest.

What is the physiological significance of activating the Ca^{2+} channels by hyperpolarization? We view control by voltage as integrating the ABA signal with the prevailing transport "poise" of the membrane (17). One consequence of raising $[Ca^{2+}]_i$ is to reduce current through inward-rectifying K^+ channels while activating Cl^- channels (9, 10) to drive the plasma membrane positive of E_K for solute loss and stomatal closure. However, if

Ca^{2+} channel activation functions to trigger a rise in $[Ca^{2+}]_i$ for membrane depolarization when the voltage is well negative of E_K, the same $[Ca^{2+}]_i$ rise must be superfluous when the voltage is already positive of E_K and, hence, biased for solute loss. Thus, the dual effects of voltage and ABA on the Ca^{2+} channel ensures that the $[Ca^{2+}]_i$ "signature" correctly reflects cellular needs for osmotic solute loss.

In conclusion, we have identified a low-conductance Ca^{2+} channel at the plasma membrane of *Vicia* guard cells that is selective for Ca^{2+} (and Ba^{2+}) over K^+ and Cl^-. We show that channel activation is stimulated by increasing $[Ba^{2+}]$ outside and suppressed by raising $[Ca^{2+}]_i$ above physiological resting values. Ca^{2+} channel opening is strongly promoted by membrane hyperpolarization and by ABA, consistent with a role for the channel in triggering increases in $[Ca^{2+}]_i$ that lead to stomatal closure. ABA evokes damped oscillations in channel activity, and the Ca^{2+} channel retains its sensitivity to ABA even in excised membrane patches, indicating that the essential elements for ABA perception, signal transduction, and Ca^{2+} channel control are retained intact on the membrane.

We thank Gerhard Thiel and Alexander Grabov for comments on the manuscript. This work was supported in part by the Biotechnology and Biological Sciences Research Council Grants P09640, C10234, and P09561, and European Community Biotech Grant CT96-0062. D.H. was a Sainsbury Ph.D. Student.

1. Sanders, D., Brosnan, J. M., Muir, S. R., Allen, G., Crofts, A. & Johannes, E. (1994) *Biochem. Soc. Symp.* 183–197.
2. Bootman, M. D. & Berridge, M. J. (1996) *Curr. Biol.* **6,** 855–865.
3. Taylor, L. P. & Hepler, P. K. (1997) *Annu. Rev. Plant Physiol. Mol. Biol.* **48,** 461–491.
4. Knight, H., Trewavas, A. J. & Knight, M. R. (1996) *Plant Cell* **8,** 489–503.
5. Hammond-Kosack, K. E. & Jones, J. D. G. (1996) *Plant Cell* **8,** 1773–1791.
6. Ehrhardt, D. W., Wais, R. & Long, S. R. (1996) *Cell* **85,** 673–681.
7. Ritchie, S. & Gilroy, S. (1998) *New Phytol.* **140,** 363–383.
8. Bush, D. S. (1993) *Plant Physiol.* **103,** 7–13.
9. Blatt, M. R. & Grabov, A. (1997) *Physiol. Plant.* **100,** 481–490.
10. Ward, J. M., Pei, Z. M. & Schroeder, J. I. (1995) *Plant Cell* **7,** 833–844.
11. Barnes, S. A., McGrath, R. B. & Chua, N. H. (1997) *Trends Cell Biol.* **7,** 21–26.
12. McAinsh, M. R., Brownlee, C. & Hetherington, A. M. (1992) *Plant Cell* **4,** 1113–1122.
13. Grabov, A. & Blatt, M. R. (1999) *Plant Physiol.* **119,** 277–287.
14. Leckie, C. P., McAinsh, M. R., Allen, G. J., Sanders, D. & Hetherington, A. M. (1998) *Proc. Natl. Acad. Sci. USA* **95,** 15837–15842.
15. Gilroy, S., Fricker, M. D., Read, N. D. & Trewavas, A. J. (1991) *Plant Cell* **3,** 333–344.
16. Staxen, I., Pical, C., Montgomery, L. T., Gray, J. E., Hetherington, A. M. & McAinsh, M. R. (1999) *Proc. Natl. Acad. Sci. USA* **96,** 1779–1784.
17. Grabov, A. & Blatt, M. R. (1998) *Proc. Natl. Acad. Sci. USA* **95,** 4778–4783.
18. Webb, A. A. R., McAinsh, M. R., Mansfield, T. A. & Hetherington, A. M. (1996) *Plant J.* **9,** 297–304.
19. Gelli, A. & Blumwald, E. (1997) *J. Membr. Biol.* **155,** 35–45.
20. Zimmermann, S., Nurnberger, T., Frachisse, J. M., Wirtz, W., Guern, J., Hedrich, R. & Scheel, D. (1997) *Proc. Natl. Acad. Sci. USA* **94,** 2751–2755.
21. Thuleau, P., Ward, J. M., Ranjeva, R. & Schroeder, J. I. (1994) *EMBO J.* **13,** 2970–2975.
22. Pineros, M. & Tester, M. (1995) *Planta* **195,** 478–488.
23. Ding, J. P. & Pickard, B. G. (1993) *Plant J.* **3,** 83–110.
24. Blatt, M. R. & Armstrong, F. (1993) *Planta* **191,** 330–341.
25. Elzenga, J. T. M., Keller, C. P. & Van Volkenburgh, E. (1991) *Plant Physiol.* **97,** 1573–1575.
26. Barry, P. H. & Lynch, J. W. (1991) *J. Membr. Biol.* **121,** 101–117.
27. Colquhoun, D. & Sigworth, F. J. (1995) in *Single Channel Recording*, eds. Sakmann, B. & Neher, E. (Plenum, New York), pp. 397–482.
28. Horn, R. (1991) *Biophys. J.* **60,** 433–439.
29. Foehr, G., Warchol, W. & Gratzl, G. (1993) *Methods Enzymol.* **221,** 149–157.
30. Dietrich, P. & Hedrich, R. (1998) *Plant J.* **15,** 479–487.
31. Grabov, A., Leung, J., Giraudat, J. & Blatt, M. R. (1997) *Plant J.* **12,** 203–213.
32. Thiel, G. & Wolf, A. H. (1997) *Trends Plant Sci.* **2,** 339–345.
33. Hille, B. (1992) *Ionic Channels of Excitable Membranes* (Sinauer, Sunderland, MA).
34. Klusener, B. & Weiler, E. W. (1999) *Plant Physiol.* **119,** 1399–1405.
35. Chapman, E. R., An, S., Edwardson, J. M. & Jahn, R. (1996) *J. Biol. Chem.* **271,** 5844–5849.
36. Zamponi, G. W. & Snutch, T. P. (1996) *Pflügers Arch. Eur. J. Physiol.* **431,** 470–472.
37. Thiel, G., MacRobbie, E. A. C. & Blatt, M. R. (1992) *J. Membr. Biol.* **126,** 1–18.
38. McAinsh, M. R., Brownlee, C. & Hetherington, A. M. (1997) *Physiol. Plant.* **100,** 16–29.
39. McAinsh, M. R., Brownlee, C. & Hetherington, A. M. (1991) *Proc. R. Soc. London Ser. B* **243,** 195–202.
40. MacRobbie, E. A. C. (1989) *Planta* **178,** 231–241.
41. Stoeckel, H. & Takeda, K. (1995) *J. Membr. Biol.* **146,** 201–209.
42. Gelli, A., Higgins, V. J. & Blumwald, E. (1997) *Plant Physiol.* **113,** 269–279.
43. Schroeder, J. I. & Hagiwara, S. (1990) *Proc. Natl. Acad. Sci. USA* **87,** 9305–9309.
44. Fairley-Grenot, K. A. & Assmann, S. M. (1992) *J. Membr. Biol.* **128,** 103–113.
45. Berridge, M. J. (1998) *Neuron* **21,** 13–26.
46. Zhou, J. M., Olcese, R., Qin, N., Noceti, F., Birnbaumer, L. & Stefani, E. (1997) *Proc. Natl. Acad. Sci. USA* **94,** 2301–2305.
47. Vergani, P., Hamilton, D., Jarvis, S. & Blatt, M. R. (1998) *EMBO J.* **17,** 7190–7198.
48. Blatt, M. R. & Gradmann, D. (1997) *J. Membr. Biol.* **158,** 241–256.
49. Zhou, Z. A. & Neher, E. (1993) *J. Physiol. (London)* **469,** 245–273.
50. Lemtiri-Chlieh, F. & MacRobbie, E. A. C. (1994) *J. Membr. Biol.* **137,** 99–107.
51. Gradmann, D., Blatt, M. R. & Thiel, G. (1993) *J. Membr. Biol.* **136,** 327–332.